International Journal of Heat and Fluid Flow 68 (2017) 348–363

Contents lists available at ScienceDirect

International Journal of Heat and Fluid Flow

journal homepage: www.elsevier.com/locate/ijhff

Large-Eddy simulation of an impinging heated jet for a small nozzle-to-plate distance and high Reynolds number

Pierre Grenson[*,a], Hugues Deniau[b]

[a] DAAA, ONERA, The French Aerospace Lab, 92190 Meudon, France
[b] DMPE, ONERA, The French Aerospace Lab, 31000 Toulouse, France

ARTICLE INFO

Keywords:
Jet impingement
Heat transfer
Large-eddy simulation
Turbulent flow
Primary structure
Hot spot

ABSTRACT

This paper reports on the investigation of an original impinging jet configuration through a wall-resolved large-eddy simulation. The heated jet issues from a fully developed pipe flow at temperature of 130 °C and a Reynolds number based on the bulk velocity of 60000. The impinged plate is located three diameters downstream of the pipe exit. The CFD results have been validated against a specifically-created experimental database (Grenson et al., 2016). The overall statistical fields are well retrieved by the simulation both in the free jet and the wall jet region. In particular, the secondary maximum at the radial location $r/D = 2$ in the Nusselt number distribution is well predicted by the simulation. The underlying mechanisms from which the secondary maximum originates has been investigated. This analysis revealed that small-scale hot spots of strong convective heat transfer coefficient are responsible for the emergence of this secondary maximum. It is shown that the hot spots can be associated either to local unsteady "separation" of the flow or streaks-like structures above the impinging plate.

1. Introduction

The impinging jet configuration is of widespread use in industrial applications (e.g. turbine blade cooling, aircraft leading edge heating) due to the high heat transfer rate experienced by the impinged surface (Han and Goldstein, 2001). It also remains a relevant configuration for turbulence modeling and numerical simulation assessment (Zuckerman and Lior, 2006; Dewan et al., 2012) due to the variety of the flow regions that coexist (Fig. 1). In this framework, an Onera joint project has been dedicated to a particular jet impingement configuration, which was selected for its high Reynolds number $Re_D = 60000$, small nozzle-to-plate distance $H/D = 3$ and temperature difference between the heated jet ($T_j = 130$ °C) and the ambient atmosphere ($T_e = 25$ °C). Because this particular configuration had never been investigated in the past, an exhaustive experimental database has been specifically created for numerical validation purposes by Grenson et al. (2016). The goal of the present paper is to numerically investigate the flow field and heat transfer distribution of this configuration through a wall-resolved large-eddy simulation (LES).

In the last decade, several LES were carried out on impinging jet configurations. Most of these simulations (Hadžiabdić and Hanjalić, 2008; Uddin et al., 2013; Aillaud et al., 2016; Natarajan et al., 2016) dealt with a turbulent jet issuing a fully developed pipe at Reynolds number $Re_D \sim 20000$ and for a nozzle-to-plate distance $H/D = 2$. Lodato et al. (2009) performed a LES for the same nozzle-to-plate distance but a higher Reynolds number $Re_D = 70000$. Unfortunately, the used grid was to coarse to meet the requirements of a wall-resolved LES and no information about the heat transfer distribution was reported. It should be noticed that the aforementioned works were dedicated to isothermal jet configuration, for which the jet temperature T_j is identical to the ambient temperature T_e.

To the authors knowledge, the present study is the first wall-resolved LES of an impinging jet configuration at such a high Reynolds number and for a heated jet.

Since the measurements of Gardon and Akfirat (1965) and Baughn and Shimizu (1989), the Nusselt number has been shown to feature a double-peak shaped distribution for impinging configurations with a nozzle-to-plate distance less than $H/D = 4$. The first peak is located at the stagnation point while the secondary peak is generally located around the radial position $r/D = 2$. Its intensity increases with the jet Reynolds number (Lee and Lee, 1999). Various explanations about the mechanisms behind this non-monotonic distribution have been proposed, generally on the basis of unsteady numerical simulations. Hadžiabdić and Hanjalić (2008) related the secondary maximum to the reattachment of local unsteady separations of the flow, by taking up the arguments of Popiel and Trass (1991) who observed such separations experimentally. The unsteady separation in impinging flows was first characterised by Didden and Ho (1985). It results from the

* Corresponding author.
E-mail address: pierre.grenson@onera.fr (P. Grenson).

http://dx.doi.org/10.1016/j.ijheatfluidflow.2017.09.014
Received 11 May 2017; Received in revised form 18 September 2017; Accepted 25 September 2017
Available online 06 November 2017
0142-727X/

Nomenclature

$\mathbf{q}$	heat flux vector (Wm^{-2})
$\mathbf{U}$	velocity vector (m/s)
Nu_D	Nusselt number (-)
Pr_t	Turbulent Prandtl number (-)
Re_D	Reynolds number (-)
St_D	Strouhal number (-)
c_p	thermal capacity at constant pressure ($Jkg^{-1}K^{-1}$)
c_v	thermal capacity at constant volume ($Jkg^{-1}K^{-1}$)
D	pipe diameter (m)
E	total energy (Jkg^{-1})
e	internal energy (Jkg^{-1})
f	frequency (Hz)
H	impingement height (m)
h	convective heat transfer coefficient ($Wm^{-2}K^{-1}$)
k_f	fluid thermal conductivity ($Wm^{-1}K^{-1}$)
p	pressure (Pa)
q_c	convective heat transfer (Wm^{-2})
T	temperature (K)
t	time (s)
T_τ	friction temperature (K)
T_{aw}	adiabatic wall temperature (K)
T_e	ambient temperature (K)
T_w	wall temperature (K)
u_x, u_r, u_θ	cylindrical velocity components (ms^{-1})
u_τ	friction velocity (ms^{-1})
U_j	jet bulk velocity (ms^{-1})
x, r, θ	cylindrical coordinates (m,m,rad)

Greek symbols

Δt	time step (s)
Δ	spatial discretisation (m)
δ_ω	vorticity thickness (m)
η	effectiveness (-)
μ	molecular viscosity ($kgm^{-1}s^{-1}$)
ν	kinematic viscosity (m^2s^{-1})
ρ	density (kgm^{-3})
τ	viscous stress tensor (Nm^{-2})
τ_c	characteristic time (s)
τ_w	wall friction (Nm^{-2})

Operators

$< \ >$	time-averaged quantity
$< \ >_{az.}$	azimuthally-averaged quantity
$^+$	wall unit
RMS	root-mean-square

interaction of the large-scale vortices generated in the free jet, often referred to as primary structures, with the plate. Flow separation is promoted by the adverse pressure gradient encountered in the vicinity these primary structures. This process eventually leads to the emergence of counter-rotating vortices, so-called secondary structures, which are advected along the plate as the primary structure progresses downstream. On the basis of the Reynolds analogy between heat and momentum transfer, Popiel and Trass (1991) and Hadžiabdić and Hanjalić (2008) related the dip between the two Nusselt number peaks to the heat transfer decrease induced by this kind of flow separation.

In their large-eddy simulation, Uddin et al. (2013) did not observe any unsteady separation but noticed the emergence of small spots of high convective heat transfer coefficient, referred as “hot spots”, in the region of the secondary maximum. Those spots are convected as the primary structure travels along the plate. By means of a direct numerical simulation of an impinging jet at $Re_D = 10000$ and $H/D = 2$, Dairay et al. (2015) showed that the hot spots are related to the instability of the secondary structures (unsteady separation). Thanks to an analysis of higher-order statistics from their LES, Aillaud et al. (2016) highlighted that the most probable event in the vicinity of the secondary maximum location is a cold fluid flux towards the plate, which leads to heat flux enhancement.

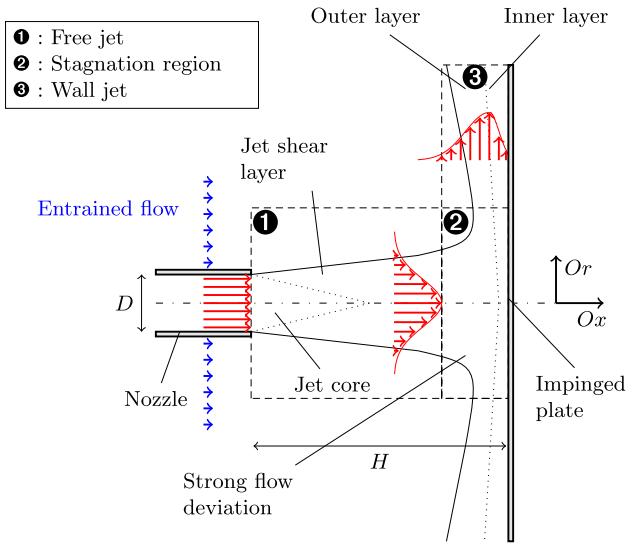

Fig. 1. Schematic description of a round jet impinging on a flat plate.

The purpose of the present work is to highlight which mechanisms take place for a high Reynolds number impinging jet which exhibits a well-pronounced secondary maximum.

The present paper is organized as follows. First, the computational setup is presented (Section 2). Next the simulation results are validated against the experimental database (Section 3). Finally, the full 3D time-resolved data from the simulation are analysed to get insight into the mechanisms related to the heat transfer distribution on the plate (Section 4).

2. Computational setup

The computational domain, sketched in Fig. 2(a), models the experimental configuration. It consists of a cylindrical domain connected to a circular pipe of diameter D. The impinged plate is represented by a disk of diameter $12D$ located $3D$ downstream of the pipe exit. Due to its large external diameter of $2.25D$, the complete nozzle geometry is also taken into account. The ambient domain is included up to $3D$ upstream of the pipe exit. The origin of the orthogonal coordinate system is located at the pipe outlet center. The jet axis is along the x direction and is taken as positive in the jet mean direction. The radial direction r is oriented along the plate.

2.1. Governing equations

The flow dynamics is governed by the compressible Navier–Stokes equations, expressed in their conservative form herebelow:

$$\frac{\partial \rho}{\partial t} + \mathrm{div}(\rho \mathbf{U}) = 0 \tag{1}$$

$$\frac{\partial (\rho \mathbf{U})}{\partial t} + \mathrm{div}(\rho \mathbf{U} \otimes \mathbf{U} + p\mathbf{I} - \tau) = 0 \tag{2}$$